Pflugers Arch - Eur J Physiol
DOI 10.1007/s00424-014-1495-1

Protein kinase C theta (PKCθ) modulates the ClC-1 chloride channel activity and skeletal muscle phenotype: a biophysical and gene expression study in mouse models lacking the PKCθ

Giulia Maria Camerino · Marina Bouchè · Michela De Bellis · Maria Cannone · Antonella Liantonio · Kejla Musaraj · Rossella Romano · Piera Smeriglio · Luca Madaro · Arcangela Giustino · Annamaria De Luca · Jean-François Desaphy · Diana Conte Camerino · Sabata Pierno

Received: 20 December 2013 / Revised: 2 March 2014 / Accepted: 5 March 2014

Abstract In skeletal muscle, the resting chloride conductance (gCl), due to the ClC-1 chloride channel, controls the sarcolemma electrical stability. Indeed, loss-of-function mutations in ClC-1 gene are responsible of myotonia congenita. The ClC-1 channel can be phosphorylated and inactivated by protein kinases C (PKC), but the relative contribution of each PKC isoforms is unknown. Here, we investigated on the role of PKCθ in the regulation of ClC-1 channel expression and activity in fast- and slow-twitch muscles of mouse models lacking PKCθ. Electrophysiological studies showed an increase of gCl in the PKCθ-null mice with respect to wild type. Muscle excitability was reduced accordingly. However, the expression of the ClC-1 channel, evaluated by qRT-PCR, was not modified in PKCθ-null muscles suggesting that PKCθ affects the ClC-1 activity. Pharmacological studies demonstrated that although PKCθ appreciably modulates gCl, other isoforms are still active and concur to this role. The modification of gCl in PKCθ-null muscles has caused adaptation of the expression of phenotype-specific genes, such as calcineurin and myocyte enhancer factor-2, supporting the role of PKCθ also in the settings of muscle phenotype. Importantly, the lack of PKCθ has prevented the aging-related reduction of gCl, suggesting that its modulation may represent a new strategy to contrast the aging process.

Keywords Skeletal muscle · PKCθ · ClC-1 chloride channel · Electrophysiology · Gene expression · Phenotype · Aging

Electronic supplementary material The online version of this article (doi:10.1007/s00424-014-1495-1) contains supplementary material, which is available to authorized users.

G. M. Camerino · M. De Bellis · M. Cannone · A. Liantonio · K. Musaraj · R. Romano · A. De Luca · J.-F. Desaphy · D. C. Camerino · S. Pierno (✉)
Section of Pharmacology, Department of Pharmacy & Drug Sciences, University of Bari - Aldo Moro, 70125 Bari, Italy
e-mail: sabata.pierno@uniba.it

M. Bouchè · P. Smeriglio · L. Madaro
Section of Histology and Medical Embryology, Department of Anatomy, Histology, Forensic Medicine & Orthopedics, Sapienza University of Rome, Rome, Italy

A. Giustino
Department of Biomedical Sciences and Human Oncology, University of Bari, Medical School, Bari, Italy

Present Address:
L. Madaro
IRCCS Fondazione Santa Lucia Epigenetics & Regenerative Pharmacology, Via del Fosso di Fiorano, 64, 00143 Rome, Italy

Present Address:
P. Smeriglio
Department Orthopaedic & Surgery, Stanford University, 300 Pasteur Dr, Edwards Bldg. R166, Stanford, CA 94305-534, USA

Abbreviations

PKCθ	Protein kinase C theta
PKCα	Protein kinase C alpha
gCl	Chloride conductance
gK	Potassium conductance
EDL	Extensor digitorum longus
Sol	Soleus
WT	Wild type
CN	Calcineurin
MEF2	Myocyte enhancer factor-2

Published online: 20 March 2014

Introduction

Skeletal muscle sarcolemma is characterized by a large resting conductance for chloride ions (gCl) important for its function [6]. Several studies demonstrate that gCl is sustained by the chloride channel (ClC-1), since the pharmacological inhibition or reduced expression of this channel results in a reduction of gCl [10, 26, 37, 42, 51]. Voltage-gated ClC-1 muscle chloride channel is a member of the CLC channel family. It allows chloride ion permeation across the sarcolemma, and its open probability increases with membrane depolarization, thus leading to repolarization and maintenance of the resting potential. The pivotal role of ClC-1 chloride channel in determining muscle function is clear in the myotonia congenita, a rare inherited disorder characterized by muscle membrane hyperexcitability, due to loss-of-function mutations in *CLCN1* gene [25]. A lower expression and activity of ClC-1 characterize the postural slow-twitch muscles with respect to the fast ones, thus contributing to the higher excitability and better resistance to fatigue which is typical of the slow fibers [12, 36]. Resting gCl is also abnormally reduced in skeletal muscle during aging process [42, 38].

It has been found that in skeletal muscle, the ClC-1 channel is regulated by a calcium and phospholipid dependent protein kinase C (PKC) and that its activation contributes to maintain a low gCl in slow-twitch muscles with respect to the fast ones [44]. However, PKC activation has been also found to be responsible for ClC-1 malfunction observed in senescent muscle and in statin drug-induced myopathy [42, 41]. Pharmacological activation of PKC, by the application of phorbol esters, decreases the resting gCl in fast muscle fibers of mouse, rat, and goat [5, 6, 56] and reduces chloride currents supported by the ClC-1 channel in a mammalian cell line [45]. The effect of phorbol esters is mediated by the phosphorylation of the ClC-1 channels [11, 21]. In contrast, the application of chelerythrine, inhibitor of PKC activity, induces an increase in the resting gCl in soleus (Sol) muscle, demonstrating the pivotal role of PKC in the inactivation of ClC-1 channels in basal conditions [44, 13]. Accordingly, chelerythrine or staurosporine, another PKC inhibitor, had a slight effect on resting gCl in rat fast muscle, in which ClC-1 channels are basically fully active and maintain the high gCl typical of fast muscles [43]. Since the resting gCl controls the electrical threshold of the sarcolemma, variation of the gCl amplitude modulates muscle excitability and, in turn, the response of the myofiber to specific nerve stimulus. Recent studies have also elegantly demonstrated the role of the PKC in the modulation of the first phase of the action potential through the inhibition of ClC-1, showing that muscle activity is associated with a downregulation of gCl [37].

PKC family of serine/threonine protein kinases is widely distributed in different tissues, where they regulate numerous cellular functions. This family is classified into three groups on the basis of the arrangement of their regulatory domains: the conventional calcium- and phospholipid-dependent cPKCs (α, β, and γ), the novel calcium-independent nPKCs (δ, ε, η, and θ), and the atypical calcium- and phospholipid-independent aPKCs (ι, ζ, and λ). Different PKC isoforms are expressed in skeletal muscle, including the novel isoform PKCθ. Actually, PKCθ is the nPKC isoform predominant in skeletal muscle, where it mediates various cellular responses required for complete histogenesis, differentiation, and homeostasis of skeletal muscle [9, 19, 23, 27, 29, 30, 34, 48, 54, 60]. Immunohistochemical studies in skeletal muscle showed the presence of PKCθ in the neuromuscular junction suggesting an important role in the development and function of the neuromuscular synapse [19].

Although the PKCθ is predominantly expressed in skeletal muscle, whether it has a role in the regulation of ClC-1 activity is still unknown. Our previous studies have demonstrated [44] reduced expression of PKCθ and other isoforms (i.e., α, ε) in rat skeletal muscle during unloading. Interestingly, the gCl is also highly sensible to disuse condition and its modification represents one of early events in phenotype transition [13, 39]. The aim of the present study was to verify whether PKCθ plays a role in the regulation of the ClC-1 channel and of muscle phenotype. In concomitance, we evaluated the influence of the other PKC isoforms present in skeletal muscle. Thus, we measured ClC-1 channel expression and activity in extensor digitorum longus (EDL) and in soleus (Sol) muscles, as well as the expression level of several genes involved in the regulation of muscle phenotype, in two different models of PKCθ-null mouse models: the PKCθ knockout model (KO), in which the PKCθ gene was inactivated in all cells [53] and the mPKCθ-K/R (K/R) transgenic model, in which a dominant-negative mutant inactive form of PKCθ is expressed under the control of a muscle-specific promoter and prevails over the endogenous one [48]. Finally, to clearly address the influence of PKCθ in causing aging-related alteration of gCl and muscle function, we measured ionic conductances and excitability parameters in skeletal muscle of senescent PKCθ-null mice.

Methods

Animal model

PKCθ knockout (KO) mice were kindly provided by Dan Littman (New York University, New York, NY, USA). In these mice, the gene-encoding PKCθ was inactivated in all cells of the body, as described previously [53]. The mPKCθ-K/R (K/R) transgenic mice were generated as previously described [48]. These mice express a PKCθ kinase dead mutant form which acts as dominant negative, specifically in muscle. C57BL6 wild-type (WT) mice (Charles River) were

used as control. The animals were housed in the department-accredited animal facility. The experiments have been performed in accordance with the Italian Guidelines for the use of laboratory animals, which conforms with the European Union Directive for the protection of experimental animals (2011/63/EU) and received approval from the Italian Health Department. Accordingly, during the experiments, all efforts were made to minimize suffering.

Experimental plan

Six- to nine-month-old transgenic (initially weighing 30 g) and wild-type (WT) (initially weighing 30 g) mice as well as 30- to 33-month-old transgenic and WT (weighing 27–31 g) mice (Charles River Laboratories, Calco, Italy) were housed individually in appropriate cages in an environmentally controlled room. All mice had water ad libitum and received 8 g a day of standard rodent chow (Charles River, 4RF21). Three to seven animals for each group were used for the experiments. Soleus (Sol) and Extensor Digitorum Longus (EDL) muscles were removed from mice deeply anesthetized by intraperitoneal injection of urethane (1.2 g/kg body weight) and used to perform the electrophysiological experiments or the FURA-2 cytofluorimetric experiments. The contralateral Sol and EDL muscles were also removed in the same conditions, frozen in liquid nitrogen and stored at −80 °C for messenger RNA (mRNA) and protein expression measurements. EDL muscles were also stored for histochemical staining. After surgery, animals were euthanized by an overdose of urethane.

Resting ionic conductances and excitability parameters measured by the two intracellular microelectrodes technique

EDL and Sol muscles were dissected from wild-type and transgenic animals, immediately placed in a muscle containing bath immersed in normal or chloride-free physiological solution maintained at 30 °C, and perfused with 95 % O_2/5 % CO_2 [11, 44, 40]. The normal physiological solution contained (in mM) NaCl 148, KCl 4.5, $CaCl_2$ 2.0, $MgCl_2$ 1.0, $NaHCO_3$ 12.0, NaH_2PO_4 0.44, glucose 5.5 (pH 7.2). The chloride-free solution was prepared by equimolar substitution of methylsulfate salts for NaCl and KCl and nitrate salts for $CaCl_2$ and $MgCl_2$. The cable parameters of myofiber sarcolemma were determined from the electrotonic potentials elicited by square wave hyperpolarizing current pulse of 100-ms duration, using two intracellular microelectrodes in current-clamp mode, as previously described [11, 44, 40]. From the values of input resistance, space constants and time constant and assuming a myoplasmic resistivity of 140 Ωcm, the fiber diameter (dcalc), the membrane resistance (Rm), and the total membrane capacitance (Cm) were then calculated. The reciprocal of Rm, from each fiber in normal physiological solution was assumed to be the total membrane conductance (gm) and the same parameter measured in chloride-free solution was considered to be the potassium conductance (gK). The mean chloride conductance (gCl) was estimated as the mean gm minus the mean gK [11, 44, 40].

The excitability characteristics of the sampled fibers were determined by recording the intracellular membrane potential response to a square-wave constant (100 ms) current pulse. In each fiber, the membrane potential was set by a steady holding current to −80 mV before passing the depolarizing pulses. By increasing the amplitude of the pulse, we were able to elicit first a single action potential, from which the AP (amplitude of action potential, in mV), Ith (threshold current, in nA), and Lat (latency of action potential, delay from the beginning of the current pulse to the onset of an action potential at threshold, in ms) were calculated. By further increasing current intensity in the same fiber, a train of action potentials (N spikes) was then generated [44].

Chelerythrine (Tocris Bioscience, Bristol, UK) 1 μM was applied in vitro on EDL and Sol muscles dissected from WT, KO, and K/R mice, and the electrophysiological measures were done after 30 min incubation. Similarly, the effects of fluvastatin (Calbiochem, Milan, Italy) 50 μM and simvastatin (Tocris) 10 μM in vitro application were recorded in EDL or Sol muscle fibers after 30 min incubation.

Fluorescence measurements of resting intracellular Ca^{2+} concentration

Fluorescence measurements were performed on small bundles of five to ten fibers lengthwise dissected from mice EDL and Sol muscles, as described elsewhere [15]. The muscle fibers were incubated with the fluorescent calcium probe fura-2 for 45–60 min at 22 °C in physiological solution containing 5 μM of the acetoxymethyl ester (AM) form of the dye mixed to 10 % (*v*/*v*) Pluronic F-127 (Molecular Probes, Leiden, The Netherlands). A QuantiCell 900 integrated imaging system (VisiTech International Ltd) was used to acquire pairs of background-subtracted images of the fura-2 fluorescence emission (510 nm) excited at 340 and 380 nm. The equation used to transform fluorescence ratio in $[Ca^{2+}]i$ values was $[Ca^{2+}]i=(R-R\min)/(R\max-R)\cdot K_D\cdot\beta$, where R is the ratio of fluorescence excited at 340 nm to that excited at 380 nm; K_D=145 nM; β, Rmin, and Rmax were determined in situ in ionomycin-permeabilized muscle fibers [15].

Western blot analysis

EDL and Sol muscles were dissected from 7-month-old WT and $PKC\theta^{-/-}$ mice (2/genotype), and homogenized in ice-cold H-buffer containing 20 mM Tris (pH 7.5), 2 mM EDTA, 2 mM EGTA, 250 mM sucrose, 5 mM dithiothreitol, leupeptin at 200 mg/ml, Aprotinin at 10 mg/ml, 1 mM phenylmethylsulfonyl fluoride, and 0.1 % Triton X-100 (all

from Sigma-Aldrich, St. Louis, MO, USA), as previously described [30]. The obtained homogenate was disrupted by sonication, incubated for 30 min on ice with repeated vortexing, and then centrifuged at 15,000×*g* for 15 min. The pellet was discarded, and the supernatant was used for Western blot analysis. An equal amount of protein from each sample was loaded onto 10 % SDS-polyacrylamide gels and transferred to a nitrocellulose membrane (Schleicher & Schuell, Dassel, Germany). The membranes were then incubated with the appropriate primary antibodies. Alkaline phosphatase (ALP)-conjugated goat anti-mouse IgG (Roche Applied Science, IN, USA) or ALP-conjugated goat anti-rabbit IgG (Zymed Laboratories, South San Francisco, CA, USA) were used as secondary antibodies, and immunoreactive bands were detected using CDP-STAR solution (Roche Applied Science), according to the manufacturer's instructions. Densitometric analysis was performed using Aida 2.1 Image software (Raytest, Straubenhardt, Germany). The following primary antibodies were used: the anti-myosin heavy chain fast or slow (Sigma), the anti-PKC-α, −ε, −θ, and the anti-phospho^{Thr538} PKCθ (Cell Signaling) [30].

Isolation of total RNA, reverse transcription and real-time PCR

Sol and EDL muscles were snap frozen in liquid nitrogen soon after removal and stored at −80 °C until use. For each muscle sample, total RNA was isolated by RNeasy Fibrous Tissue Mini Kit (Qiagen C.N. 74704) and quantified by using a spectrophotometer (ND-1000 NanoDrop, Thermo Scientific). To performed reverse transcription, for each sample, 400 ng of total RNA, was added to 1 μl dNTP mix 10 mM each (Roche, NC 11277049001), 1 μl Random Hexamers 50 μM (Life Technologies C.N. n808-0127) and incubated at 65 °C for 5 min. Afterward, 4 μl 5X First Standard Buffer (Life Technologies C.N. Y02321), 2 μl 0,1 M DTT (Life Technologies C.N. Y00147), and 1 μl Recombinant RNasin Ribonuclease Inhibitor 40 U/μl (Promega, C.N. N2511) were added and incubated at 42 °C for 2 min. To each solution, it was added 1 μl SuperScript II Reverse Transcriptase 200 U/μl (Life Technologies C.N. 18064–014) and incubated at 25 °C for 10 min, at 42 °C for 50 min and at 70 °C for 15 min. Real-time PCR was performed in triplicate using the Applied Biosystems Real-time PCR 7500 Fast system, MicroAmp Fast Optical 96-Well Reaction Plate 0.1 mL (Life Technologies C.N. 4346906) and MicroAmp Optical Adhesive Film (Life Technologies C.N. 4311971). Each reaction was carried in triplicate on as single plex reaction. The setup of reactions consisted of 8 ng of cDNA, 0.5 μl of TaqMan Gene Expression Assays (Life Technologies), 5 μl of TaqMan Universal PCR master mix No AmpErase UNG (2×) (Life Technologies C.N. 4324018), and Nuclease-Free Water not DEPC-Treated (Life Technologies C.N. AM9930) for a final volume of 10 μl. Under the following RT-TaqMan-PCR conditions: step 1: 95 °C for 20 s; step 2: 95 °C for 3 s; and step 3: 60 °C for 30 s, steps 2 and 3 were repeated 40 times. The results were compared with relative standard curve obtained by 5 points of 1:4 serial dilutions. The mRNA expression of the genes was normalized to the best housekeeping genes hypoxanthine phosphoribosyltransferase 1 (HPRT1) selected from beta-actin (Actb) and HPRT1. TaqMan Hydrolysis primer and probe gene expression assays were ordered with the following assay IDs: (Hprt1) ID assay: Mm00446968_m1; muscle RING-finger protein-1 (MURF1) ID assay: Mm01185221_m1; histone deacetylase 5 (HDAC5) ID assay: Mm01246076_m1; myostatin (MSTN) ID assay: Mm01254559_m1; nuclear factor of activated T-cells, cytoplasmic1 (Nfatc1) ID assay: Mm00479445_m1; nuclear factor of kappa light polypeptide gene enhancer in B-cells 1 (Nfkb1) ID assay: Mm00476361_m1; pyruvate kinase, muscle 2 (Pkm2) ID assay: Mm00834102_gH; myosin heavy chain 1 (MHC1) ID assay: Mm00600555_m1; insulin receptor substrate 1 (IRS1) ID assay: Mm01278327_m1; myocyte enhancer factor 2D (MEF2D) ID assay: Mm00504931_m1; calcineurin (CN) ID assay: Mm01317678_m1. For Actin beta we found following primer For: 5′-CCAGATCATGTTTGAG ACCTTCAA-3′, primer Rev: 5′-CATACAGGGACAGCAC AGCCT-3′, probe: VIC-ACC CCA GCC ATG TAC GTA-MGB. For chloride channel one (ClC-1) found following primer For: 5′-TCATGCTCGGTGTCCGAAA-3′, primer Rev: 5′-CAGGCGGTGCTTAGCAAGA-3′, probe: 6-FAM-ATT GGC TGA GAC ACT TGT-MGB [40].

NADH-tetrazolium reductase histochemical staining of skeletal muscle sections

For NADH-tetrazolium reductase (NADH-TR) staining, EDL cryosections were incubated for 15 min with NADH-TR reaction solution in 0.2 M Tris pH 7.4 (Sigma-Aldrich, St. Louis, MO, USA) at 37 °C, as described [2, 28]. The percentage of NADH-TR-positive fibers was determined by counting all fibers in the entire section (three sections/muscle from three mice), and a mean was calculated for each mouse. With NADH-TR staining, three types of fibers were observed: unstained, moderately stained, and darkly stained. Fibers that were darkly stained were classified as NADH-TR positive.

Statistical analysis

To compare the various experimental groups of animals, statistical analysis was performed using two-way analysis of variance (ANOVA) followed by ad hoc Bonferroni's *t* test. When needed, comparison of means between two experimental conditions was done using unpaired Student's *t*-test. A *P* value minor to 0.05 was considered statistically significant.

Results

Evaluation of the expression of different PKC isoforms in skeletal muscle of WT and PKCθ-KO mice by WB analysis

As first, the expression level and activation of PKCθ was analyzed in Sol and EDL muscles from WT mice and in the KO. As shown in Fig. 1, PKCθ is highly expressed in both muscles, and a comparable fraction of it is phosphorylated. As expected, no PKCθ immunoreactivity was detectable in muscles derived from PKCθ-KO mice. Among the other isoforms analyzed, PKCα and PKCε are similarly expressed in both muscles of WT mice. Lack of PKCθ resulted in a slight increase in PKCα expression in both muscles, as compared to WT, while PKCε expression was slightly decreased in Sol muscle. We had already shown that the expression of PKCα and other PKC isoform were not modified in skeletal muscle of mPKCθ-K/R transgenic mice [48].

Modification of resting membrane chloride and potassium conductance (gCl and gK) in Sol and EDL muscles of PKCθ-null mice

We found that the resting gCl was higher in skeletal muscle of PKCθ-KO mice with respect to WT. In particular, this parameter was significantly increased by 38.0±3.8 % and by 13.0±2.9 % in Sol and EDL muscles, respectively, as compared to WT (Fig. 2b and Fig. 3b). Also a significant increase of the resting gK was observed in EDL muscle of KO mice with respect to WT (Fig. 3b). However, resting gK was not significantly modified in Sol muscle (Fig. 2b). Representative traces of the electrotonic potential (measured at a distance of 0.05 mm between the two microelectrodes) evoked in normal physiological solution to measure resting membrane conductance (gm) and in chloride-free solution to measure resting gK from Sol and EDL muscles of KO and WT mice are shown in Fig 2a and Fig. 3a, respectively. As detailed in the methods section, the resting gCl was calculated as the difference between gm and gK. Slightly minor effects were found in mPKCθ-K/R transgenic (K/R) mice as compared to WT. Indeed, gCl was significantly increased by 21.0±6.8 % in Sol muscle and by only 6.0±3.7 % in EDL muscle of these mice (Supplementary Fig. S1b and S2b). Resting gK was only slightly increased in EDL muscle and unchanged in Sol muscle of K/R mice (Supplementary Figs. S1b and S2b). Representative traces of electrotonic potential from which gCl was calculated in Sol and EDL muscle of K/R mice are shown in the Supplementary Figs. S1a and S2a.

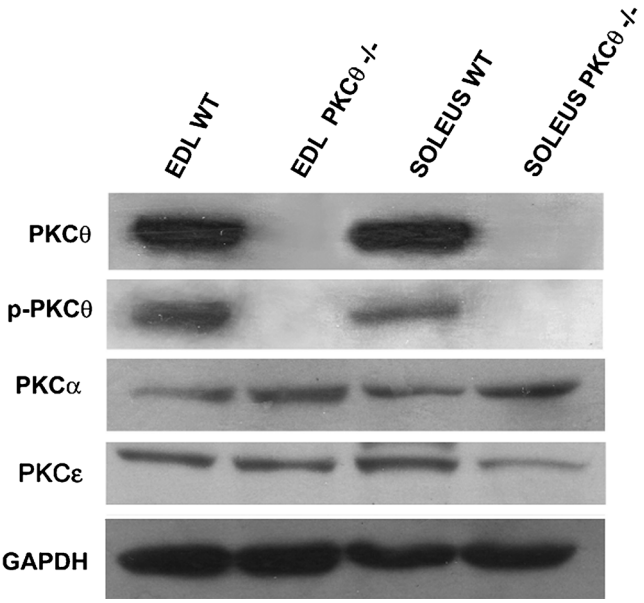

Fig. 1 Expression of nPKC specific isoforms in soleus (*Sol*) and extensor digitorum longus (*EDL*) muscles of wild-type (WT) and PKCθ-knockout ($PKC\theta^{-/-}$) transgenic mice. Western blot analysis of protein extracts was prepared from muscle cells. The blots were reacted with antibodies specific for the different nPKC isoforms, as indicated. An anti-GAPDH antibody was used to normalize the blot

Effects of chelerythrine and statins in vitro application on resting gCl in Sol and EDL muscles of PKCθ null mice

Chelerythrine, a known PKC inhibitor, was applied in vitro to Sol and EDL muscle fibers dissected from WT, PKCθ-KO, and mPKCθ-K/R mice. As shown in the Fig. 4a, the PKC inhibitor induced a significant increase in the resting gCl in Sol muscle of WT mice by 63.0±8.1 %. In muscle of PKCθ-KO mice, being the basal resting gCl already higher than that of WT, chelerythrine in vitro application increased it by 25.8±3.7 %, reaching the same value reached in WT muscle in the presence of chelerythrine. A similar significant increase of resting gCl (by 31.5±7.4 %) was observed by addition of chelerythrine on Sol muscle of mPKCθ-K/R mice (Supplementary Fig. S3a). In the EDL muscle, the increase of gCl due to chelerythrine in vitro application was less marked (Fig. 4a). In particular, it was significant only in the muscle of the WT mice. In muscles of KO as well as in K/R mice, chelerythrine application slightly increased gCl, reaching the same value reached in WT muscle in the presence of chelerythrine (Fig. 4a and Supplementary Fig. S3a). In accord with the minor effect of chelerythrine on gCl in EDL muscle, we have previously demonstrated [44] that the application of chelerythrine in fast muscles produces smaller effects because ClC-1 channels, in normal resting conditions, are mainly in the active state.

We also evaluated the role of PKCθ in statin-induced gCl decrease. In fact, we had previously shown that in vitro application of fluvastatin to EDL/Sol muscle fibers of Wistar rats decreases the resting gCl through the activation of PKC [41]. We observed here that fluvastatin in vitro application to Sol and EDL muscles of WT as well as of KO mice significantly decreased gCl with respect to the value measured in the

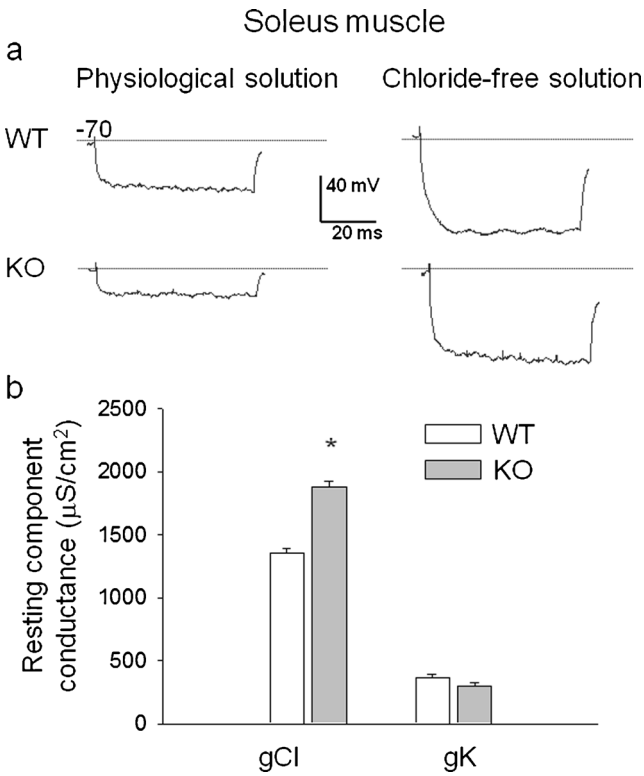

Fig. 2 Resting chloride conductance (*gCl*) and resting potassium conductance (*gK*) measured in soleus (*Sol*) muscle of wild-type (*WT*) and PKCθ-knock-out (*KO*) mice. **a** Representative traces of the electrotonic potentials recorded in Sol muscle fibres by standard two microelectrodes technique at 0.05 mm distance between electrodes, in response to hyperpolarizing square-wave current pulse. The electrotonic potential recorded in normal physiological solution allows to measure membrane resistance Rm and its reciprocal, the total membrane conductance (gm). The electrotonic potential recorded in chloride-free solution allows to measure the potassium conductance (gK). The chloride conductance (gCl) is the mean gm minus the mean gK. **b** Measure of resting component conductances for Cl^- and K^+. Each *bar* represents the mean value±S.E.M. of 15–57 fibers from 3–7 animals. Statistical analysis was performed using ANOVA followed by Bonferroni's *t*-test. Significantly different (*asterisk*) with respect to WT (at least $P<0.05$)

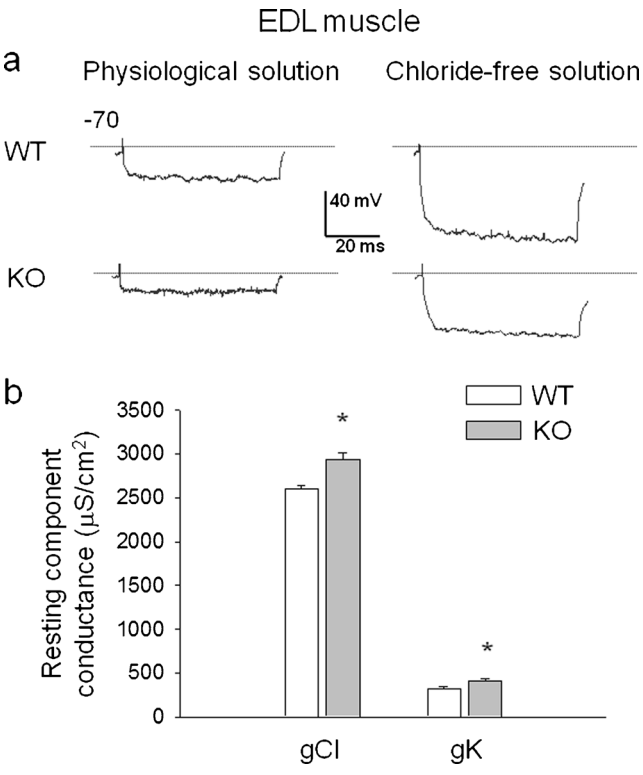

Fig. 3 Resting chloride conductance (*gCl*) and resting potassium conductance (*gK*) measured in extensor digitorum longus (*EDL*) muscle of wild-type (*WT*) and PKCθ-knock-out (*KO*) mice. **a** Representative traces of the electrotonic potentials recorded in EDL muscle fibres by standard two microelectrodes technique at 0.05 mm distance between electrodes, in response to hyperpolarizing square-wave current pulse. The electrotonic potential recorded in normal physiological solution allows to measure of membrane resistance Rm and its reciprocal, the total membrane conductance (gm). The electrotonic potential recorded in chloride free solution allows to measure the gK. The gCl is the mean gm minus the mean gK. **b** Measure of resting component conductances for Cl^- and K^+. Each *bar* represents the mean value±S.E.M. of 15–57 fibers from 3–7 animals. Statistical analysis was performed using ANOVA followed by Bonferroni's *t*-test. Significantly different (*asterisk*) with respect to WT (at least $P<0.05$)

absence of the drug (Fig. 4b). Similarly, the in vitro application of simvastatin, another hypolipidaemic compound, produced a significant reduction of gCl both in Sol and EDL muscles of mPKCθ-K/R mice (Supplementary Fig. S3b).

Modification of excitability parameters in Sol and EDL muscles of PKCθ-null mice

Since gCl is determinant for muscle excitability and its perturbation affects these events, in parallel, we measured the excitability parameters in Sol and EDL muscle fibers from PKCθ-null mice, both KO and K/R mice and compared it to WT. Thus, we measured the amplitude of the action potential (AP), the current necessary for the triggering of one action potential (Ith), the latency of the action potential (Lat), and the maximum number of action potentials elicited by raising the intensity of a long-duration pulse (N spikes). As shown in Fig. 5a, both Sol and EDL muscle fibers from KO mice were less excitable with respect to WT animals. Indeed, a significant decrease in the Lat in Sol and in EDL muscle fibers was observed in KO mice, as compared to WT. A significant decrease in the N spikes was also observed in EDL muscle fibers of KO mice (Fig. 5a). No significant differences were observed in AP, and Ith in KO mice, as compared to WT (Supplementary Fig. S4). Similar but smaller effects were found in K/R mice (Supplementary Fig. S5 and S6). At this regard, it is known that a modification of gCl exceeding 30 % of control is required before significant alteration of membrane excitability can be observed [1, 8]. Accordingly, the modification of the excitability parameters agreed with the observed reduction of gCl. A representative experiment is shown in the Fig. 5b, where the first action potential as well

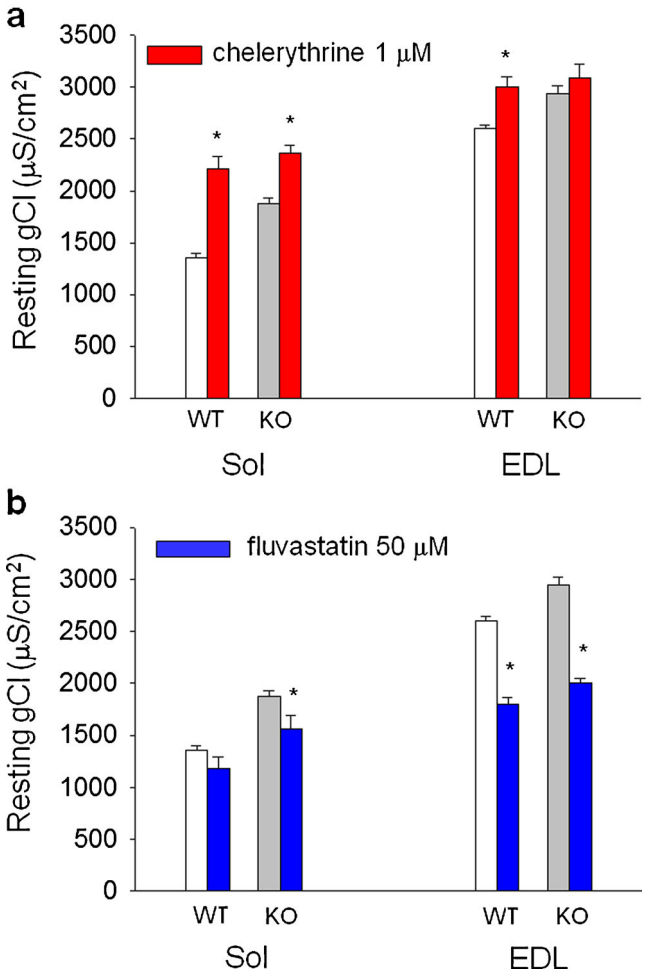

Fig. 4 Effects of chelerythrine and statin in vitro application on resting chloride conductance (*gCl*) measured in soleus (*Sol*) and extensor digitorum longus (*EDL*) muscles of wild-type (*WT*) and PKCθ-knock-out (KO) mice. **a** Chelerythrine (1 μM), a PKC inhibitor, was applied acutely on muscle bath 30 min before the electrophysiological recordings in all the experimental conditions. Each *bar* represents the mean value± S.E.M. of 10–27 fibers from 3–7 animals. Statistical analysis was performed using ANOVA followed by Bonferroni's *t*-test. Significantly different (*asterisk*) with respect to the value recorded in the absence of chelerythrine (at least $P<0.05$). **b** Fluvastatin (50 μM), previously demonstrated to stimulate PKC activity [39], was applied acutely on muscle bath 30 min before the electrophysiological recordings in all the experimental conditions. Each *bar* represents the mean value±S.E.M. of 9–21 fibers from 3–7 animals. Statistical analysis was performed using ANOVA followed by Bonferroni's *t*-test. Significantly different (*asterisk*) with respect to the value recorded in the absence of drug (at least $P<0.05$)

as the maximum number of spikes was measured in the EDL muscle of WT and KO mice.

The effects of in vitro application of chelerythrine on the excitability parameters were also investigated. The PKC inhibitor significantly reduced the Lat of AP in Sol muscle of WT mice and not significantly in EDL muscle of WT (Supplementary Fig. S5 and S6). However, it had slight effects on the Lat and on the N spikes in Sol and EDL of KO mice, being the value similar to that measured in the absence of the compound (Fig. 5a). Slight changes of the excitability parameters were also induced by chelerythrine in Sol and EDL muscle of K/R mice (Supplementary Fig. S5 and S6).

Modification of calcium homeostasis in Sol and EDL muscles of PKCθ-null mice

Because the resting cytosolic calcium concentration depends on muscle phenotypes, we evaluated its concentration in Sol and EDL muscles dissected from WT and PKCθ-null mice, both KO and K/R mice. As expected, the resting cytosolic calcium concentration was higher in the Sol muscle, as compared to the EDL, in WT animals [15]. Interestingly, this parameter was significantly reduced in the Sol muscle of both PKCθ-KO (Fig. 6) and PKCθ-K/R (Supplementary Fig. S7) mice, when compared to WT mice. Also in the EDL muscle the lack of expression or activity of PKCθ resulted in a reduction of cytosolic calcium concentration, although the difference was not significant (Fig. 6 and Supplementary Fig. S7).

Gene expression modification in Sol and EDL muscles of PKCθ-null mice

Since gCl is sustained by the ClC-1 channel, we measured mRNA expression in muscles of PKCθ-null mice, both KO and K/R mice. We found that ClC-1 expression was not significantly modified in EDL and Sol muscles of PKCθ-KO and in mPKCθ-K/R animals, as compared to WT (Fig. 7 and Supplementary Fig. S8).

To further characterize the adaptation changes in gene expression due to the lack of PKCθ in Sol and EDL muscles, the mRNA level of selected genes involved in muscle plasticity and atrophy, as well as in glucose homeostasis was also explored (Fig. 7 and Supplementary Fig. S8). We found that the mRNA level of the slow myosin heavy chain type-1 (MHC-1) was slightly increased in Sol of K/R mice and slightly decreased in EDL of both KO and K/R mice. The expression of calcineurin (CN), a protein phosphatase involved in the activation of several muscle-specific slow gene promoters, was significantly increased only in Sol muscle of KO mice and decreased in EDL muscle of the same animal model. Myocyte enhancer factor 2d (MEF2d), another important modulator of muscle gene expression, was significantly increased in Sol muscle and was significantly decreased in EDL muscle of both KO and K/R mice. We also evaluated the mRNA level of the histone deacetylase 5 (HDAC5), and of the nuclear factor of activated T cells (NFAT), the translocation of which is also implicated in muscle plasticity. HDAC5 was not modified in Sol and EDL muscles of both animal models and NFAT was significantly increased in the Sol of KO mice. A slight decrease of NFAT was observed in EDL muscle of either KO or K/R mice (Fig. 7 and Supplementary Fig. S8).

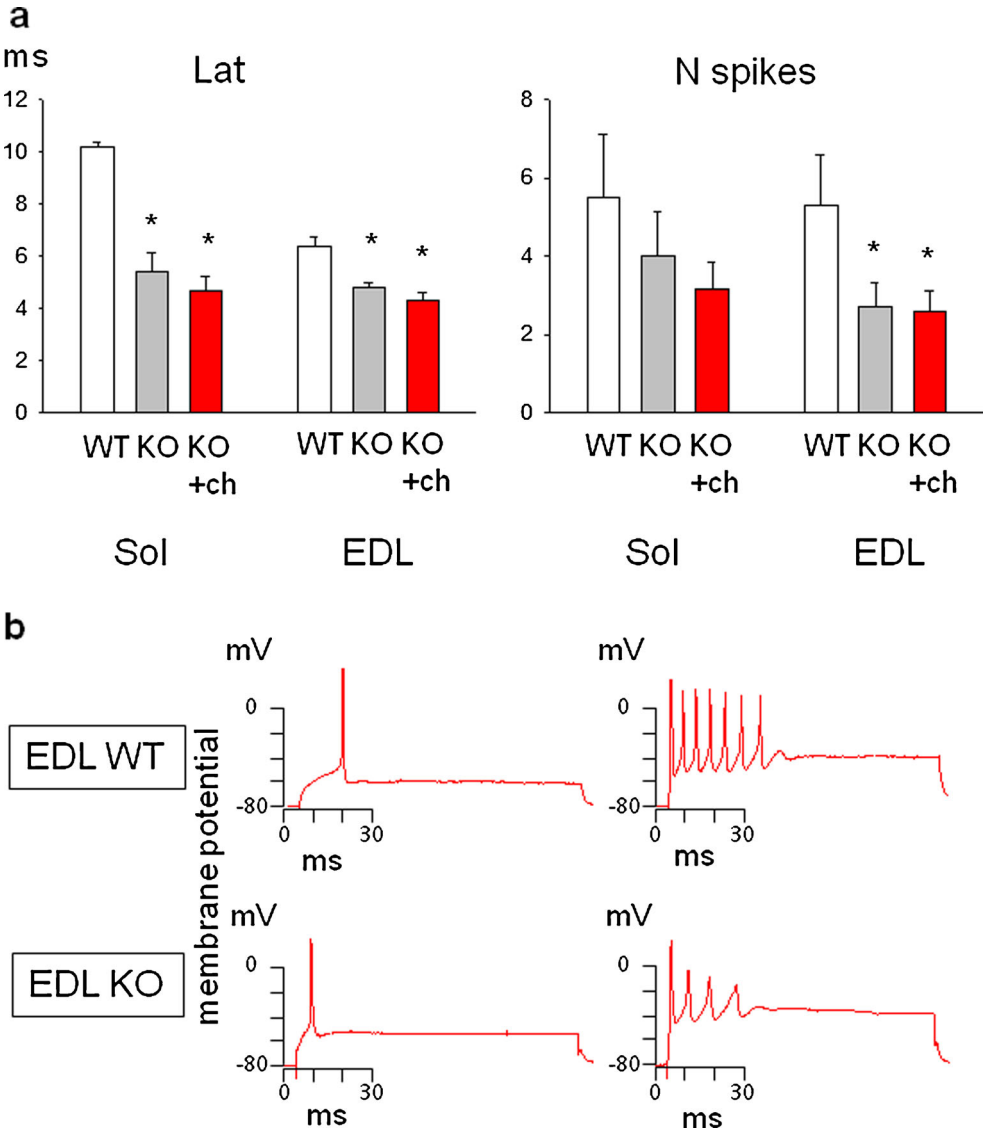

Fig. 5 Excitability parameters measured in soleus (*Sol*) and extensor digitorum longus (*EDL*) muscles of wild-type (*WT*) and PKCθ-knock-out (*KO*) mice. **a** The latency (*Lat*) of the first action potential and the maximum number of spikes (N spikes) elicitable with a maximal stimulation were measured. The effects of 1 μM chelerythrine (indicated as *ch*) in vitro application on skeletal muscle of PKCθ-KO mice were also measured. Each bar represents the mean value±S.E.M. of 8–21 fibers from 3–7 animals. Statistical analysis was performed using ANOVA followed by Bonferroni's *t*-test. Significantly different (*asterisk*) with respect to WT (at least $P<0.05$). **b** Representative example of the first action potential elicited by threshold current as well as of the maximum number of spikes elicitable by increasing the amplitude of the current measured in the EDL muscle of PKCθ KO with respect to WT mice. Action potentials were recorded in skeletal muscle fibers using two-microelectrode current clamp method

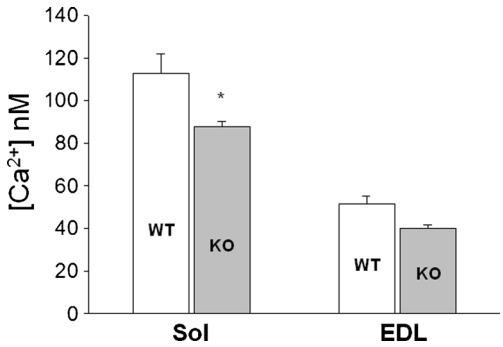

Fig. 6 Resting cytosolic calcium concentration (restCa) measured in soleus (*Sol*) and extensor digitorum longus (*EDL*) muscles of wild-type (*WT*) and PKCθ-knock-out (*KO*) mice. RestCa was measured in skeletal muscle by using fura-2 fluorescence method. Each *bar* represents the mean value±S.E.M. of 9–55 fibers from 3–7 animals. Statistical analysis was performed using ANOVA followed by Bonferroni's *t*-test. Significantly different (*asterisk*) with respect to WT (at least $P<0.05$)

We also found a modification of the expression of the piruvate kinase M2 (PKM2) and insulin receptor substrate 1 (IRS1) involved in glucose homeostasis. In fact, a significant increase of PKM2 was found in Sol muscle of both KO and K/R mice. However, no significant modifications were found in the EDL muscle. The mRNA expression of IRS1 was significantly reduced only in the EDL muscle of KO and K/R mice (Fig. 7 and Supplementary Fig. S8).

Since the PKCθ may be involved in the regulation of catabolic pathways [49] and the change of phenotype may be associated to muscle atrophy, the expression of atrophy genes were also analyzed. However, no modification of the atrogene MuRF1 and of myostatin mRNA was found (Fig. 7 and Supplementary Fig. S8). Moreover, the nuclear factor kappa-light-chain-enhancer of activated B cells (NF-κB), which can be activated during muscle atrophy [3], was, in

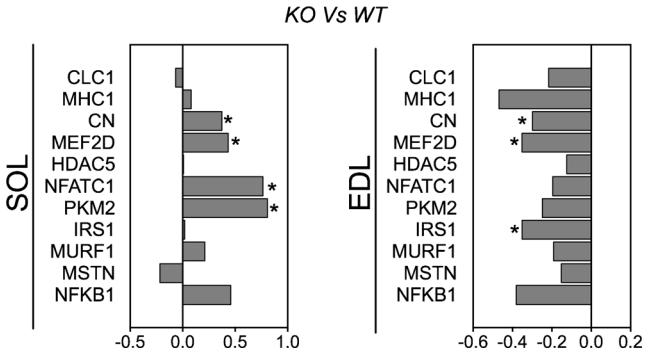

Fig. 7 Gene expression modification in soleus (*Sol*) and extensor digitorum longus (*EDL*) muscles of wild-type (*WT*) and PKCθ-knock-out (*KO*) mice. Transcript levels were determined by real-time PCR for selected genes indicated with the abbreviation on the *left*. The numbers on the *abscissa* indicate the fold change in gene expression normalized for housekeeping gene. The *bars* indicate the fold change in gene expression in KO vs. WT. The number of animals examined was 3–7 for each group. Statistical analysis was performed using ANOVA followed by Bonferroni's *t*-test. Significantly different (*asterisk*) with respect to WT (at least $P<0.05$). *ClC-1* ClC-1 chloride channel, *MyHC1* myosin heavy chain type-1, *CN* calcineurin, *MEF2D* myocyte enhancer factor 2d, *HDAC5* histone deacetylase; NFAT, nuclear factor of activated T cells; PKM2, piruvate kinase M2; IRS1, insulin receptor substrate 1, *MURF-1* muscle RING-finger protein-1, *MSTN* myostatin, *NFKB1*, nuclear factor kappa-light-chain-enhancer of activated B cells

contrast, significantly reduced in EDL muscle of K/R mice (Fig. 7 and Supplementary Fig. S8).

Evaluation of the oxidative fibers percentage by NADH-TR staining in EDL muscles of PKCθ-null mice

We stained EDL transverse sections from WT and PKCθ-null$^{-/-}$ mice to verify whether lack of PKCθ determined any change in the percentage of NADH-TR-positive fibers, as a result of fiber type modification. As shown in Fig. 8, the percentage of dark stained (oxidative) fibers was significantly decreased in muscle derived from PKCθ$^{-/-}$ mice, as compared to that derived from WT mice, according to a change of phenotype towards the fast one.

The age-related modification in resting gCl and excitability parameters was prevented in EDL muscle of senescent PKCθ-null mice

Since the resting gCl is reduced in skeletal muscle of aged subjects and this reduction was partially attributed to an increase of PKC activity, we recorded the resting gCl in EDL muscle of 30–33-month-old PKCθ-KO mice. As expected, a significant reduction of the resting gCl by 80 % was found in EDL muscle of senescent WT animals with respect to the adults (Fig. 9a). On the other hand, the gCl was significantly higher in the EDL of senescent PKCθ-KO mice with respect to age-matched WT, toward the adult value. In contrast, the resting gK remained higher than that of WT in aged muscle (Fig. 9b). Accordingly to gCl reduction, the EDL muscle of aged WT animals was more excitable with respect to the adults, being the max number of spikes 12.8±1.2 (n=9) and 5.9±1.0 (n=10), respectively. This parameter was ameliorated in EDL muscle of senescent PKCθ-KO mice being more similar to that of the adults (8.3±1.4, n=12). Representative traces of action potentials (AP) are showed in Fig. 9c.

Discussion

In mammalian skeletal muscle, the protein kinase C (PKC) controls the ClC-1 channel activity and the related chloride conductance. Different PKC isoforms are expressed in this tissue. The PKCα, a Ca^{2+}-activated and phospholipid-dependent protein kinase, is the most expressed isoform among the conventional PKC isoforms (α, β, γ) in mouse skeletal muscle. This isoform was found to be more elevated in EDL muscle than in Sol muscle [22]. Experiments using the calcium ionophore A23187 and dantrolene, a calcium channel blocker, suggested the cPKCα, as the isoform controlling the resting gCl [11, 24, 37, 41]. Also the Ca^{2+}-independent PKCθ, a member of the group of the novel PKCs, is highly expressed in skeletal muscle, but its specific role in the ClC-1 regulation was not established. Our previous studies suggest an important role for this isoform in the progression of the slow-to-fast transition typical of muscle disuse [9, 44].

Identification of the putative role of PKCθ isoform in skeletal muscle function by the use of animal models

The results of the present study, obtained by using two different mouse models lacking PKCθ, give us important information on the role of this isoform in signal transduction pathway in skeletal muscle. These models are critically important to address PKC function since specific inhibitors are not available. Indeed, both models have been successfully used to investigate the role of PKCθ on muscle function. For instance, it has been found that PKCθ is important for muscle regeneration, as it is upregulated after freeze-induced injury and myofiber regeneration is impaired in PKCθ-null mice [29]. It has been also demonstrated that PKCθ ablation ameliorates muscular dystrophy in the mdx mouse model [30].

Here, we found that, in addition to cPKCα, also the PKCθ has a role in the regulation of chloride channel activity and of skeletal muscle function. The lack of PKCθ in the KO mice and the inhibition of its activity in the K/R mice [48] moves the resting gCl to higher values with respect to the WT. The increase of resting gCl accounts for the lack of the PKCθ inhibitory effect on the ClC-1 channel. This effect has been observed either in Sol or EDL muscles of transgenic mice, being more pronounced in the slow-twitch muscle, probably because the PKC isoforms present in this muscle are basically more active [37, 44].

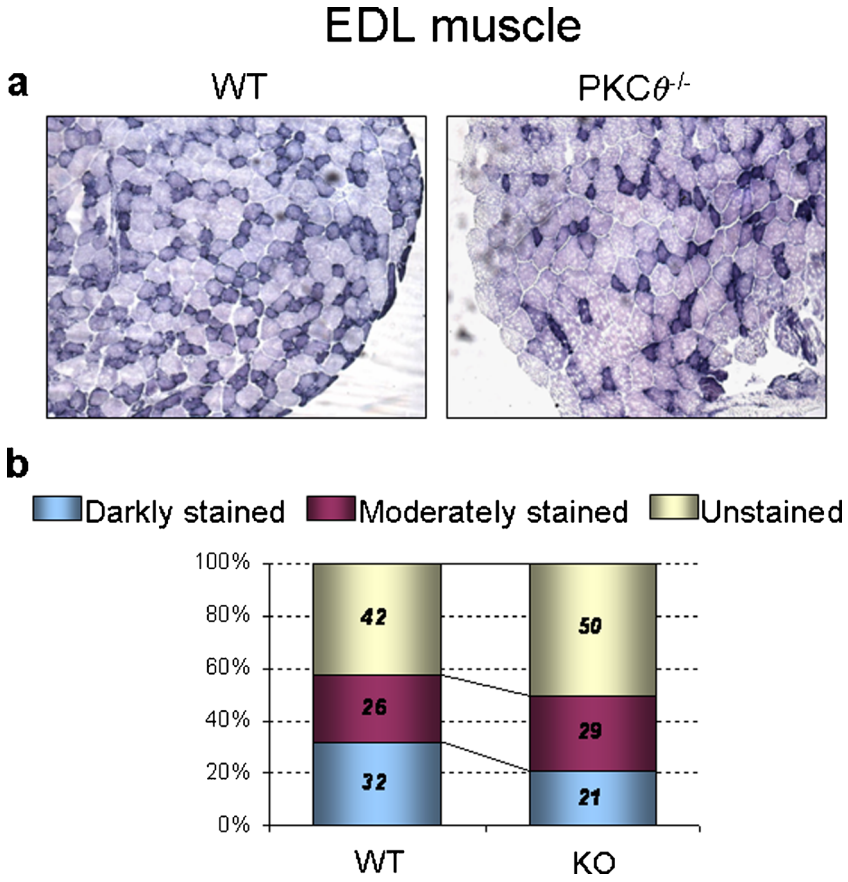

Fig. 8 Lack of PKCθ reduces the number of oxidative/NADH-TR positive fibers in EDL muscle. **a** NADH-TR histochemistry analysis of EDL muscle derived from 6-month-old WT or PKCθ$^{-/-}$ mice. Representative pictures are shown. **b** Mean number of NADH-TR positive (darkly stained) or negative (unstained, moderately stained) fibers in EDL muscle from WT or PKCθ$^{-/-}$ mice (three sections/muscle from three mice/genotype)

Although the results obtained from the two animal models go in the same direction, the effects are slightly lower in the transgenic K/R mice with respect to the KO mice. This can be due to the presence of the endogenous form of PKCθ in muscle, although it was showed to be 2- or 3-fold lower with respect to the mutated one [48]. Although the mutant protein can easily compete for the activity of the wild-type enzyme, our results suggest that the endogenous PKCθ may conserve a partial activity on ClC-1. It cannot be fully excluded that the lower effect observed in K/R mice may stem from the lack of PKCθ inhibition in non-muscular tissues. However, the PKCθ isoform is far less expressed in non-muscular tissues, including the nervous system [33, 35], thus its inhibition in these tissues may have only marginal effect on skeletal muscle properties.

Cross-talk between PKCα and PKCθ and modulation of muscle electrophysiological parameters and phenotype

It is worth to note that the application of chelerythrine to skeletal muscle of PKCθ-null mice further increases resting gCl, demonstrating that other PKC isoforms are able to modulate ClC-1 activity in the absence of PKCθ. After application of chelerythrine, the gCl reached a similar maximal value in WT, KO and K/R mice, showing that gCl cannot be further increased. This is in accord with the observation that modification of gCl in PKCθ-null mice is not related to the modification of ClC-1 mRNA expression. However, the maximal gCl value was different between Sol and EDL muscle types, being lower in Sol muscle, because of the lesser chloride channel expression typical of this muscle phenotype [39]. Muscle excitability, index of muscle function, is also reduced in the transgenic mice and chelerythrine in vitro application further reduced it, although not markedly, according to the increase of resting gCl. The in vitro application of two different hypocholesterolemic drugs, already demonstrated to reduce gCl by stimulating the calcium-dependent PKC [24, 41], further reduced gCl, again corroborating the finding that different PKC isoforms modulate gCl. In this case, the effect was more pronounced in the fast EDL muscle, where an elevated concentration of inactive PKC is present in the cytosol and can be recruited in the membrane when needed. We demonstrated that the expression of the other PKC isoforms was not strongly modified in PKCθ-lacking mice. In addition to gCl, a significant increase of resting gK was observed in the EDL of KO mice, and a similar trend was also observed in the K/R mice. This suggests a PKCθ-mediated modulation of some potassium channels that are typically expressed in the fast-twitch

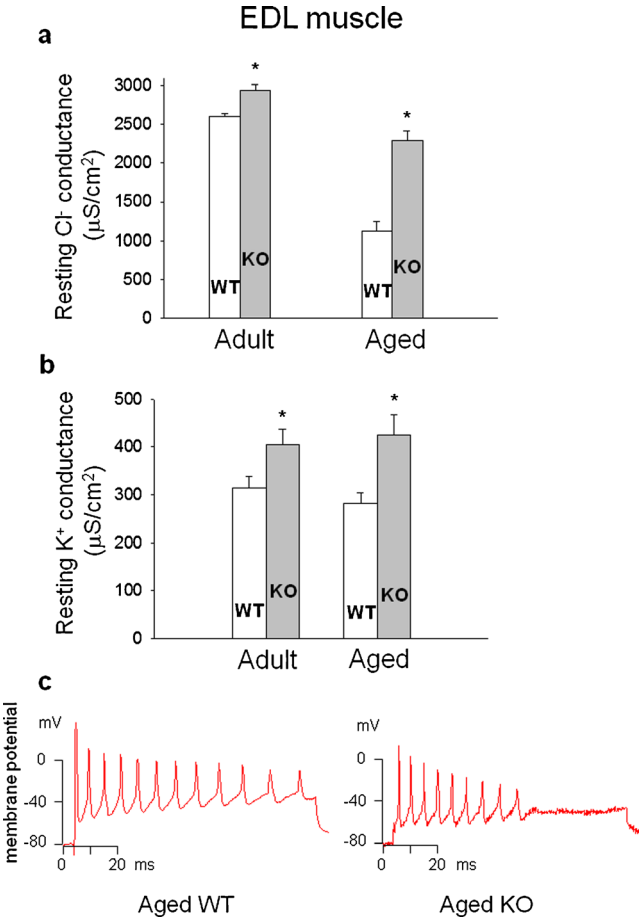

Fig. 9 Resting chloride conductance (*gCl*) (**a**) and resting potassium conductance (*gK*) (**b**) measured in extensor digitorum longus (*EDL*) muscles of 30–33 month-old aged wild-type (*WT*) and 30–33 month-old aged PKCθ-knock-out (*KO*) mice. Each *bar* represents the mean value±S.E.M. of 15–30 fibers from three animals. Statistical analysis was performed using ANOVA followed by Bonferroni's *t*-test. Significantly different (*asterisk*) with respect to WT (at least $P<0.05$). **c** Representative example of the maximum number of action potentials elicitable by raising the intensity of a depolarizing current pulse measured in the EDL muscle of aged WT and aged PKCθ-KO mice

muscles [55, 57]. The intracellular resting calcium (restCa) was also decreased in muscles of PKCθ-lacking models preferentially in slow-twitch muscles, accordingly with the change of phenotype toward the fast one. The increase of gCl and consequent excitability reduction is likely responsible for the change in phenotype through a reduced release of calcium from sarcoplasmic reticulum and reduced stimulation of calcineurin [4, 39, 44, 47]. The change in phenotype probably includes the modulation of expression and activity of proteins involved in Ca^{2+} homeostasis, which set the restCa level.

PKCθ-mediated pathways involved in the regulation of muscle gene program

It has been demonstrated that PKCθ cooperates with CN in the activation of molecular pathways inducing slow muscle specific gene program [9]. A current hypothesis suggests that tonic motor nerve activity modifies the intracellular free calcium and CN. PKCθ is localized at the neuromuscular junction and its expression is likely regulated by nerve function [48] suggesting a role in mediating nerve–muscle interaction [19, 20]. CN and NFAT act as sensors of nerve activity and control slow muscle promoter activation [31] through the increase of their molecular target MEF2 [58]. Thus, the increase of MEF2 shifts gene expression towards the oxidative phenotype. The increase of diacylglycerol (DAG) may constitute a switch signal for PKCθ resulting in the modulation of both MEF2 transcriptional complex formation and HDACs nucleus/cytoplasm shuttling [7, 9, 32]. Interestingly, a phenotype transition was also observed in conditions where the resting gCl was altered; the genetic inhibition of ClC-1 in myotonic muscles leads to fast-to-slow phenotype transition [59], while the increased gCl in Sol muscle after disuse is accompanied by a slow-to-fast phenotype transition [44, 39]. It is worth to note that an abnormal increase of MEF2 has been observed in myotonic muscle fibers, a pathological condition characterized by a low gCl [59], suggesting a correlation between these parameters. Thus, we hypothesized that the increase of resting gCl in PKCθ-null mice may have a role in the modification of muscle phenotype, and we analyzed the expression of factors that contribute to muscle phenotype development.

In mice lacking PKCθ, we found a reduction of CN, MEF2, and NFAT expression in the fast-twitch EDL muscle. This is in accord with a shift toward a fast-to-faster phenotype, which correlates with a reduction of the slow-type MHC and, with an increase of gCl as well as with a decrease in excitability. These findings suggest a role of PKCθ in the modulation of parameters involved in the phenotype settings although the ClC-1 channel mRNA expression was not modified. A more important transition was expected in Sol muscle of mice lacking PKCθ. Such a phenotype shift is indeed documented by the gCl increase, excitability and restCa decrease. Surprisingly, the expression of CN, MEF2, and NFAT appeared to be increased in mice lacking PKCθ. We suppose that this may constitute a compensatory effect aimed at the preservation of slow phenotype in the soleus muscle of PKCθ-KO mice, in which the reduced excitability may result in a severe loss of function. However, this tentative appeared to be insufficient to maintain the slow phenotype, probably because PKCθ is lacking totally. On the basis of these results, we can hypothesize that the interruption of PKCθ-mediated signaling pathways in the transgenic mice, modify ClC-1 activity and in consequence muscle phenotype. In favor of this hypothesis, we previously found that the increase in gCl precedes the slow-to-fast transition during muscle disuse [39].

Also, a reduction of IRS1 expression has been found in the EDL muscle of the PKCθ-lacking mice, accordingly with

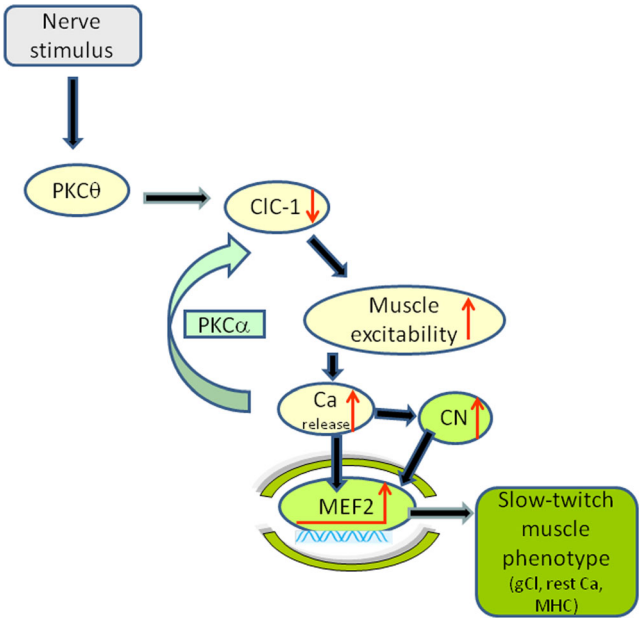

Fig. 10 Diagram of the hypothesized mechanism by which *PKCθ* affects the *ClC-1* chloride channel activity and the phenotype settings in skeletal muscle. PKCθ activation is responsible for the phosphorylation and closure of ClC-1 channel, producing a reduction of gCl and an increase of sarcolemma excitability. In consequence PKCθ is responsible for the increase of calcium (*Ca*) release from sarcoplasmic reticulum and activation of calcineurin (*CN*) and myocyte enhancer factor 2 (*MEF2*), both of them contributing to the setting of slow phenotype gene program [44]. A reduction of gCl is often correlated with a fast to slow phenotype transformation in several forms of myotonia [6, 25, 59] as well in pathophysiological conditions such as aging [4, 42]. A cross-talk between PKCθ and *PKCα* (activated by Ca increase) was also hypothesized in the control of ClC-1 activity. As detailed in the text, we found a modification of this pathway in our animal model lacking PKCθ activity, which resembles the modification observed during muscle disuse [44] in which the PKCθ-mediated inhibitory control of ClC-1 is lost and a phenotype transition toward the fast one occurs

muscle phenotype transition [46, 52]. Moreover, as MEF2 is important for GLUT4 expression in skeletal muscle, MEF2 reduction in the EDL may modify glucose homeostasis in fast muscle of PKCθ-lacking mice with an impairment of function. These results corroborate the hypothesis that PKCθ plays a role in the regulation of glucose metabolism and insulin action in skeletal muscle, although the molecular mechanism remains to be clarified [48]. Interestingly, the lack of PKCθ increases the expression of PKM2, a glycolytic enzyme involved in proliferative processes, in Sol muscle. It was found that the upregulation of this enzyme induces changes in type 1 muscle fibers associated with increased glucose consumption, reduced oxidative metabolism, and muscle atrophy during pathological states such as myotonic dystrophy [16, 18]. However, we found that the expression of MuRF1, a muscle atrogene, and of myostatin, a negative regulator of myoblast proliferation and differentiation [14], was not modified in Sol muscle lacking PKCθ although the increase of PKM2.

Concluding remarks

These results provide the first evidence that PKCθ contributes to the fine tuning of the muscle ClC-1 chloride channel activity and sarcolemma excitability, as well as of specialized myofiber phenotype either in slow-twitch or in fast-twitch muscle fibers. The abolition of PKCθ expression or activity, in the animal models used here, causes the shift of muscle phenotype toward the fast one and can contribute to a modification of phenotype-specific function. Our hypothesis is that the ClC-1 channel is under the control of at least two PKC isotypes, i.e., PKCθ and the PKCα, that are regulated by distinct input and/or modulators. This double regulation can be due to different reasons. For instance it is known that the PKCα is localized in the the cytosol and is recruited under stimulus, while the PKCθ is present in the sarcolemma [33] and can be immediately available for cell needs. In addition, since the PKCθ is regulated by nerve activity, it can directly influence muscle fiber phenotype. It has been also proposed a functional cross-talk for the integration of signaling networks in cells, in terms of opposite role of the two different isoforms in the regulation of fast and slow phenotype [17, 49, 50]. Figure 10 summarizes all the results obtained in this study and hypothesizes the sequence of events involved in the mechanism by which PKCθ controls muscle ClC-1 channel and muscle phenotype. A modification of this pathway was found in our animal model lacking PKCθ activity, similarly to that observed during muscle disuse [44] in which the PKCθ-mediated inhibitory control of ClC-1 is lost and a slow-to-fast phenotype transition takes place, especially in soleus muscle. Interestingly, the lack of PKCθ prevents the abnormal reduction of gCl observed in skeletal muscle during aging process and maintains a normal sarcolemma excitability. This result suggests the possibility to slow sarcopenia process by counteracting the reduction of gCl through pharmacological modulation of PKCθ. In conclusion, this study strongly indicates PKCθ as a useful target for pharmacological intervention aimed at preventing and/or counteracting chloride channel malfunction and/or phenotype change.

Acknowledgments The support of ASI-OSMA is gratefully acknowledged.

References

1. Adrian RH, Bryant SH (1974) On the repetitive discharge in myotonic muscle fibres. J Physiol 240:505–515
2. Allen DL, Harrison BC, Maass A, Bell ML, Byrnes WC, Leinwand LA (2001) Cardiac and skeletal muscle adaptations to voluntary wheel running in the mouse. J Appl Physiol 90(5):1900–1908
3. Bassel-Duby R, Olson EN (2006) Signaling pathways in skeletal muscle remodeling. Annu Rev Biochem 75:19–37

4. Berchtold MW, Brinkmeier H, Müntener M (2000) Calcium ion in skeletal muscle: its crucial role for muscle function, plasticity, and disease. Physiol Rev 80:1215–1265
5. Brinkmeier H, Jockusch H (1987) Activators of protein kinase C induce myotonia by lowering chloride conductance in muscle. Biochem Biophys Res Commun 148:1383–1389
6. Bryant SH, Conte-Camerino D (1991) Chloride channel regulation in the skeletal muscle of normal and myotonic goats. Pflugers Arch 417: 605–610
7. Chang S, Bezprozvannaya S, Li S, Olson EN (2005) An expression screen reveals modulators of class II histone deacetylase phosphorylation. Proc Natl Acad Sci U S A 102:8120–8125
8. Conte-Camerino D, Tortorella V, Ferranini E, Bryant SH (1984) The toxic effects of clofibrate and its metabolite on mammalian skeletal muscle: an electrophysiological study. Arch Toxicol Suppl 7:482–484
9. D'Andrea M, Pisaniello A, Serra C, Senni MI, Castaldi L, Molinaro M, Bouché M (2006) Protein kinase C theta co-operates with calcineurin in the activation of slow muscle genes in cultured myogenic cells. J Cell Physiol 207:379–388
10. De Luca A, Conte Camerino D, Connold A, Vrbovà G (1990) Pharmacological block of chloride channels of developing rat skeletal muscle affects the differentiation of specific contractile properties. Pflugers Arch 416:17–21
11. De Luca A, Tricarico D, Pierno S, Conte Camerino D (1994) Aging and chloride channel regulation in rat fast-twitch muscle fibres. Pflugers Arch 427:80–85
12. Desaphy JF, Pierno S, Léoty C, George AL Jr, De Luca A, Camerino DC (2001) Skeletal muscle disuse induces fibre type-dependent enhancement of Na(+) channel expression. Brain 124:1100–1113
13. Desaphy JF, Pierno S, Liantonio A, De Luca A, Didonna MP, Frigeri A, Nicchia GP, Svelto M, Camerino C, Zallone A, Camerino DC (2005) Recovery of the soleus muscle after short- and long-term disuse induced by hindlimb unloading: effects on the electrical properties and myosin heavy chain profile. Neurobiol Dis 18:356–365
14. Elkina Y, von Haehling S, Anker SD, Springer J (2011) The role of myostatin in muscle wasting: an overview. J Cachex Sarcopenia Muscle 2:143–151
15. Fraysse B, Desaphy JF, Pierno S, De Luca A, Liantonio A, Mitolo CI, Camerino DC (2003) Decrease in resting calcium and calcium entry associated with slow-to-fast transition in unloaded rat soleus muscle. FASEB J 17:1916–1918
16. Gao Z, Cooper TA (2013) Reexpression of pyruvate kinase M2 in type 1 myofibers correlates with altered glucose metabolism in myotonic dystrophy. Proc Natl Acad Sci U S A 110:13570–13575
17. Gundersen K (2011) Excitation-transcription coupling in skeletal muscle: the molecular pathways of exercise. Biol Rev Camb Philos Soc 86:564–600
18. Gupta V, Wellen KE, Mazurek S, Bamezai RN (2013) Pyruvate kinase M2: regulatory circuits and potential for therapeutic intervention. Curr Pharm Des Jun 25 [Epub ahead of print]
19. Hilgenberg L, Miles K (1995) Developmental regulation of a protein kinase C isoform localized in the neuromuscular junction. J Cell Sci 108:51–61
20. Hilgenberg L, Yearwood S, Milstein S, Miles K (1996) Neural influence on protein kinase C isoform expression in skeletal muscle. J Neurosci 16:4994–5003
21. Hsiao KM, Huang RY, Tang PH, Lin MJ (2010) Functional study of CLC-1 mutants expressed in *Xenopus* oocytes reveals that a C-terminal region Thr891-Ser892-Thr893 is responsible for the effects of protein kinase C activator. Cell Physiol Biochem 25:687–694
22. Jensen TE, Maarbjerg SJ, Rose AJ, Leitges M, Richter EA (2009) Knockout of the predominant conventional PKC isoform, PKCα, in mouse skeletal muscle does not affect contraction-stimulated glucose uptake. Am J Physiol Endocrinol Metab 297:E340–E348
23. Li Y, Soos TJ, Li X, Wu J, Degennaro M, Sun X, Littman DR, Birnbaum MJ, Polakiewicz RD (2004) Protein kinase C θ inhibits insulin signaling by phosphorylating IRS1 at Ser^{1101}. J Biol Chem 279:45304–45307
24. Liantonio A, Giannuzzi V, Cippone V, Camerino GM, Pierno S, Camerino DC (2007) Fluvastatin and atorvastatin affect calcium homeostasis of rat skeletal muscle fibers in vivo and in vitro by impairing the sarcoplasmic reticulum/mitochondria Ca^{2+}-release system. J Pharmacol Exp Ther 321:626–634
25. Lossin C, George AL Jr (2008) Myotonia congenita. Adv Genet 63: 25–55
26. Lueck JD, Mankodi A, Swanson MS, Thornton CA, Dirksen RT (2007) Muscle chloride channel dysfunction in two mouse models of myotonic dystrophy. J Gen Physiol 129:79–94
27. Madaro L, Antonangeli F, Favia A, Esposito B, Biamonte F, Bouché M, Sica G, Ziparo E, Filippini A, D'Alessio A (2013) Knock down of caveolin-1 affects morphological and functional hallmarks of human endothelial cells. J Cell Biochem 114:1843–1851
28. Madaro L, Marrocco V, Carnio S, Sandri M, Bouché M (2013) Intracellular signaling in ER stress-induced autophagy in skeletal muscle cells. FASEB J 27(5):1990–2000
29. Madaro L, Marrocco V, Fiore P, Aulino P, Smeriglio P, Adamo S, Molinaro M, Bouché M (2011) PKCθ signaling is required for myoblast fusion by regulating the expression of caveolin-3 and β1D integrin upstream focal adhesion kinase. Mol Biol Cell 22: 1409–1419
30. Madaro L, Pelle A, Nicoletti C, Crupi A, Marrocco V, Bossi G, Soddu S, Bouché M (2012) PKC theta ablation improves healing in a mouse model of muscular dystrophy. PLoS ONE 7(2):e31515
31. McCullagh KJ, Calabria E, Pallafacchina G, Ciciliot S, Serrano AL, Argentini C, Kalhovde JM, Lømo T, Schiaffino S (2004) NFAT is a nerve activity sensor in skeletal muscle and controls activity-dependent myosin switching. Proc Natl Acad Sci U S A 101: 10590–10595
32. McGee SL (2007) Exercise and MEF2-HDAC interactions. Appl Physiol Nutr Metab 32:852–856
33. Meller N, Altman A, Isakov N (1998) New perspectives on PKCtheta, a member of the novel subfamily of protein kinase C. Stem Cells 16:178–192
34. Messina G, Biressi S, Monteverde S, Magli A, Cassano M, Perani L, Roncaglia E, Tagliafico E, Starnes L, Campbell CE, Grossi M, Goldhamer DJ, Gronostajski RM, Cossu G (2010) Nfix regulates fetal-specific transcription in developing skeletal muscle. Cell 140: 554–566
35. Osada S, Mizuno K, Saido TC, Suzuki K, Kuroki T, Ohno S (1992) A new member of the protein kinase C family, nPKC theta, predominantly expressed in skeletal muscle. Mol Cell Biol 12:3930–3938
36. Pedersen TH, de Paoli F, Nielsen OB (2005) Increased excitability of acidified skeletal muscle: role of chloride conductance. J Gen Physiol 125:237–246
37. Pedersen TH, Macdonald WA, de Paoli FV, Gurung IS, Nielsen OB (2009) Comparison of regulated passive membrane conductance in action potential-firing fast- and slow-twitch muscle. J Gen Physiol 134:323–337
38. Pierno S, De Luca A, Camerino C, Huxtable RJ, Camerino DC (1998) Chronic administration of taurine to aged rats improves the electrical and contractile properties of skeletal muscle fibers. J Pharmacol Exp Ther 286(3):1183–1190
39. Pierno S, Desaphy JF, Liantonio A, De Bellis M, Bianco G, De Luca A, Frigeri A, Nicchia GP, Svelto M, Léoty C, George AL Jr, Camerino DC (2002) Change of chloride ion channel conductance is an early event of slow-to-fast fibre type transition during unloading-induced muscle disuse. Brain 125:1510–1521
40. Pierno S, Camerino GM, Cannone M, Liantonio A, De Bellis M, Digennaro C, Gramegna G, De Luca A, Germinario E, Danieli-Betto D, Betto R, Dobrowolny G, Rizzuto E, Musarò A, Desaphy JF,

Camerino DC (2013) Paracrine effects of IGF-1 overexpression on the functional decline due to skeletal muscle disuse: molecular and functional evaluation in hindlimb unloaded MLC/mIgf-1 transgenic mice. PLoS ONE 8(6):e65167
41. Pierno S, Camerino GM, Cippone V, Rolland JF, Desaphy JF, De Luca A, Liantonio A, Bianco G, Kunic JD, George AL Jr, Conte Camerino D (2009) Statins and fenofibrate affect skeletal muscle chloride conductance in rats by differently impairing ClC-1 channel regulation and expression. Br J Pharmacol 156:1206–1215
42. Pierno S, De Luca A, Beck CL, George AL Jr, Conte Camerino D (1999) Aging-associated down-regulation of ClC-1 expression in skeletal muscle: phenotypic-independent relation to the decrease of chloride conductance. FEBS Lett 449:12–16
43. Pierno S, De Luca A, Desaphy JF, Fraysse B, Liantonio A, Didonna MP, Lograno M, Cocchi D, Smith RG, Camerino DC (2003) Growth hormone secretagogues modulate the electrical and contractile properties of rat skeletal muscle through a ghrelin-specific receptor. Br J Pharmacol 139:575–584
44. Pierno S, Desaphy JF, Liantonio A, De Luca A, Zarrilli A, Mastrofrancesco L, Procino G, Valenti G, Conte Camerino D (2007) Disuse of rat muscle in vivo reduces protein kinase C activity controlling the sarcolemma chloride conductance. J Physiol 584: 983–995
45. Rosenbohm A, Rüdel R, Fahlke C (1999) Regulation of the human skeletal muscle chloride channel hClC-1 by protein kinase C. J Physiol 514:677–685
46. Ryder JW, Bassel-Duby R, Olson EN, Zierath JR (2003) Skeletal muscle reprogramming by activation of calcineurin improves insulin action on metabolic pathways. J Biol Chem 278:44298–44304
47. Schiaffino S, Serrano A (2002) Calcineurin signaling and neural control of skeletal muscle fiber type and size. Trends Pharmacol Sci 23:569–575
48. Serra C, Federici M, Buongiorno A, Senni MI, Morelli S, Segratella E, Pascuccio M, Tiveron C, Mattei E, Tatangelo L, Lauro R, Molinaro M, Giaccari A, Bouché M (2003) Transgenic mice with dominant negative PKC-theta in skeletal muscle: a new model of insulin resistance and obesity. J Cell Physiol 196:89–97
49. Sneddon WB, Liu F, Gesek FA, Friedman PA (2000) Obligate mitogen-activated protein kinase activation in parathyroid hormone stimulation of calcium transport but not calcium signaling. Endocrinology 141:4185–4193
50. Steinberg SF (2008) Structural basis of protein kinase C isoform function. Physiol Rev 88:1341–1378
51. Steinmeyer K, Ortland C, Jentsch TJ (1991) Primary structure and functional expression of a developmentally regulated skeletal muscle chloride channel. Nature 354:301–304
52. Stuart CA, McCurry MP, Marino A, South MA, Howell ME, Layne AS, Ramsey MW, Stone MH (2013) Slow-twitch fiber proportion in skeletal muscle correlates with insulin responsiveness. J Clin Endocrinol Metab 98:2027–2036
53. Sun Z, Arendt CW, Ellmeier W, Schaeffer EM, Sunshine MJ, Gandhi L, Annes J, Petrzilka D, Kupfer A, Schwartzberg PL, Littman DR (2000) PKC-θ is required for TCR-induced NF-κB activation in mature but not immature T lymphocytes. Nature 404:402–407
54. Tokugawa S, Sakuma K, Fujiwara H, Hirata M, Oda R, Morisaki S, Yasuhara M, Kubo T (2009) The expression pattern of PKCθ in satellite cells of normal and regenerating muscle in the rat. Neuropathology 29:211–218
55. Tricarico D, Camerino DC (2011) Recent advances in the pathogenesis and drug action in periodic paralyses and related channelopathies. Front Pharmacol 2:8. doi:10.3389/fphar.2011.00008
56. Tricarico D, Conte Camerino D, Govoni S, Bryant SH (1991) Modulation of rat skeletal muscle chloride channels by activators and inhibitors of protein kinase C. Pflugers Arch 418:500–503
57. Webb BLJ, Hirst SJ, Giembycz MA (2000) Protein kinase C isoenzymes: a review of their structure, regulation and role in regulating airways smooth muscle tone and mitogenesis. Br J Pharmacol 130: 1433–1452
58. Wu H, Rothermel B, Kanatous S, Rosenberg P, Naya FJ, Shelton JM, Hutcheson KA, DiMaio JM, Olson EN, Bassel-Duby R, Williams RS (2001) Activation of MEF2 by muscle activity is mediated through a calcineurin-dependent pathway. EMBO J 20:6414–6423
59. Wu H, Olson EN (2002) Activation of the MEF2 transcription factor in skeletal muscles from myotonic mice. J Clin Invest 109:1327–1333
60. Zappelli F, Willems D, Osada S, Ohno S, Wetsel WC, Molinaro M, Cossu G, Bouché M (1996) The inhibition of differentiation caused by TGFβ in fetal myoblasts is dependent upon selective expression of PKCθ: a possible molecular basis for myoblast diversification during limb histogenesis. Dev Biol 180:156–164